Coastally Trapped Waves over a Double Shelf Topography(I) : Free Waves with Exponential Topography

Ig-Chan PANG
Department of Oceanography, National University of Cheju, Cheju 690-120, Korea

양향성 대륙붕의 대륙붕파(I) : 지수함수적 해저지형에서의 자유파

방 익 찬
제주대학교 해양학과

Double shelf topography allows the existence of two sets of waves propagating in opposite directons. In the case that two shelves are apart sufficiently enough, the solutions show two independent sets of waves which recover the single shelf waves. However, if the distance between two shelves is less than the Rossby deformation radius, the waves become dependent on the geometry of both shelves.

Even over a double shelf topography, shelf waves propagate with the shallow water to the right in the Northern Hemisphere. The group velocity of shelf wave has the same direction as phase velocity in the long wave case, but the opposite direction in the short wave case. Each shelf mode has a zero group velocity at some intermediate value of wave length.

Introduction

Since the advent of the continental shelf wave theory by Buchwald and Adams(1968), the theory of coastally trapped waves has gradually been established for coastal areas that lie next to a deep ocean. They have shown that the continental shelf waves are generated by the long-shore component of the wind stress. A particular lucid explanation of the generation mechanixm has been given by Gill and Schumann(1974). They derived, in the long wave limit and in the absence of friction, a first order wave equation from which the amplitude of a given mode of continental shelf waves can be determined. Brink and Allen(1978) have extended the derivation to include friction and showed that there is a frictionally induced cross-shelf phase shift as well as an alongshore decay in wave amplitude. The mode are also found to be coupled. Clarke and Van Gorder(1986) first solved the fully coupled set of wave equations by integration along the characteristics. The general properties of coastally trapped waves travelling over various monotonic depth profiles have been reviewed by LeBlond and Mysak(1978) and a general theory of these waves have been discussed by Huthnance(1975, 1978).

There are other coastal areas in which the depth of the ocean does not increase monotonically away

* 이 논문은 1989~1991 과학재단 신진연구비에 의해 연구되었음.

from the shore. The bottom slope is reversed, for example, across submarine banks and trenches. This also admits trapped waves and these waves have been investigated by Louis(1978), Mysak *et al.* (1979, 1980, 1981), and Brink(1983). The bottom slope is also reversed across a double shelf topography such as in the Yellow Sea. Although the coastally trapped waves over a double shelf topography share some of the characteristics of waes found over banks and trenches, the former differs from the latter in important dynamical ways. In spite of a basic establishment of the wave theory over a double shelf topography(Pang, 1987: Hsueh and Pang, 1989), it still needs to develop the theory for clarifying the intrinsic dynamics. The purpose of this paper is to establish the theory of the free waves over a exponential double shelf topography clearly.

Exponential bottom topography allows a simple analytical solution to the coastally trapped wave problem which can readily be compared to the results from existing theories. Thus, the first step should be to establish the theory with exponential bottom topography. We want to see if the theory recovers the familiar results for the single shelf case when the problem is reduced to that of two dynamically separate shelves. We also want to see the effects of topography, compared with a single shelf, and what the phase speeds(eigenvalues), group speeds, and eigenfunctions of the two sets of modes are like.

Field Equation and Boundary Conditions

Small pertubations to a barotropic ocean satisfy the equation

$$Hp_{xxt}+H_xp_{xt}+Hp_{yyt}+fH_xp_t+(rp_x)_x-([f^2-\omega^2]/g)p_t$$
$$=-([f^2-\omega^2]/g)p_{at}+f(Y_x-X_y) \qquad (1)$$

In this equation, x, y, t, p, g, f, r, H, p_a, X and Y refer, respectively, to cross-shelf distance, alongshore distance, time, the perturbation pressure divided by mean water density, the acceleration due to gravity, the Coriolis parameter, the bottom resistance coefficient, the water depth, the atmospheric pressure divided by the mean water density, the kinematic stresses in x and y direction at surface (the wind stress divided by the mean water density). The subscripts indicate the derivatives.

Fig. 1 shows a schematic representation of the coordinates system and the geometry of two shelves(1 and 2) of exponential depth profile and a level intervening region. For convinence, let's take the positive x direction eastward. Then, the positive y direction is northward. The bottom topography (H) can be set as

$$H(X)=\begin{cases} H_1=H_0\exp(2bx), & -B_1\leq x\leq \text{ in shelf 1} \\ H_m=H_0, & 0\leq x\leq L_m \text{ in middle area} \\ H_2=H_0\exp(-2d\{-L_m\}), & L_m\leq x\leq B_2 \text{ in shelf 2} \end{cases} \qquad (2)$$

where b and d are the bottom slope coefficients of shelves 1 and 2. The subscripts 1, 2, and m indicate shelf 1, shelf 2, and middle area, respectively.

To begin with, an intervening region is put between the two shelves, that is, the shelf 1, intervening region and shelf 2 are placed, respectively, in $-B_1\leq x\leq 0$, in $0\leq x\leq L_m$, in $L_m\leq x\leq B_2$. At the coasts, no-flux boundary conditions are applied at $x=-B_1$, B_2, where the depth is three times the Ekman layer e-folding scale (Mitchum and Clarke, 1986).

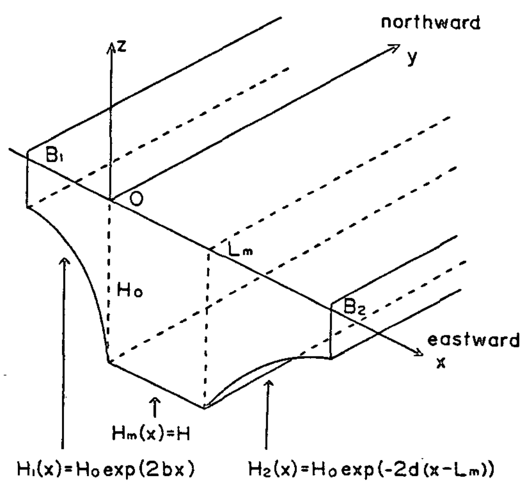

Fig. 1. Schematic representation of the coordinate system and geometry of two shelves of exponential depth profile and a level intervening region. The coordinates x, y and z refer to the cross-shelf, alongshore, and vertical directions and are oriented eastward, northward, and upward, respectively.

That is, the depth integrated cross-channel velocity component vanishes at a distance from the coast. Also, continuous pressure and continuous mass transport boundary conditions are applied at $x=0, L_m$. The applied boundary conditions are summarized as follows:

$$P_{1xt}+(r/h)p_{1x}+fP_{1y}=fY/h \quad \text{at } x=-B_1 \quad (3-1)$$
$$P_1=P_m \quad \text{at } x=0 \quad (3-2)$$
$$P_{1xt}+fP_{1y}=P_{mxt}+fP_{my} \quad \text{at } x=0 \quad (3-3)$$
$$P_m=P_2 \quad \text{at } x=L_m \quad (3-4)$$
$$P_{mxt}+fP_{my}=P_{2xt}+fP_{2y} \quad \text{at } x=L_m \quad (3-5)$$
$$P_{2xt}+(r/h)P_{2x}+fP_{2y}=fY/h \quad \text{at } x=B_2 \quad (3-6)$$

Dispersion Relation

In order to compare this result with those of existing theories, the horizontal divergence and bottom friction are not included here. The field equation (1) is reduced for non-divergent, low-frequency free waves in a frictionless barotropic flow as follows:

$$Hp_{xxt}+H_xp_{xt}+Hp_{yyt}+fH_xp_y=0 \quad (4)$$

The long-wave limit is not used here. Upon substituting for the pressure, $p=F(x)\exp(i\{\ell y+\omega t\})$, (4) yields

$$HF''+H'F'-\ell^2HF+(f/c)H'F=0 \quad (5)$$

where the 'prime' means the derivative with respect to x and $c=\omega/\ell$. (5) with the depth profiles given by (2) yields the following eigen value problem for the frictionless eigenfunction F(X):

$$F_1''+2bF_1'+(2bf/c-\ell^2)F_1=0, \quad -B_1\leq x\leq 0 \quad (6-1)$$
$$F_m''-1^2F_m=0, \quad 0\leq x\leq L_m \quad (6-2)$$
$$F_2''-2dF_2'-(2df/c+\ell^2)F_2=0, \quad L_m\leq x\leq B_2 \quad (6-3)$$

$$F_1'+(f/c)F_1=0, \quad \text{at } x=-B_1 \quad (7-1)$$
$$F_1=F_m, \quad \text{at } x=0 \quad (7-2)$$
$$F_1'=F_m', \quad \text{at } x=0 \quad (7-3)$$
$$F_m=F_2 \quad \text{at } x=L_m \quad (7-4)$$
$$F_m'=F_2', \quad \text{at } x=L_m \quad (7-5)$$
$$F_2'+(f/c)F_2=0, \quad \text{at } x=B_2 \quad (7-6)$$

where F_1, F_m and F_2 represent the eigenfunctions over, respectively, the shelf 1, intervening region and shelf 2. From (6) and (7), we get the following dispersion relation with b, d, B_1, B_2, and L_m as parameters:

$$\begin{aligned}
&(-n_1-b+\ell)\ (+n_2-d+\ell)\\
&\times\exp(-\ell L_m)\ \exp(+n_1B_1)\ \exp(-n_2\{B_2-L_m\})\\
&+(-n_1-b+\ell)\ (+n_2+d-\ell)\\
&\times\exp(-\ell L_m)\ \exp(+n_1B_1)\ \exp(+n_2\{B_2-L_m\})\\
&-(n_1-b+\ell)\ (+n_2-d+\ell)\\
&\times\exp(-\ell L_m)\ \exp(-n_1B_1)\ \exp(-n_2\{B_2-L_m\})\\
&-(+n_1-b+\ell)\ (+n_2+d-\ell)\\
&\times\exp(-\ell L_m)\ \exp(-n_1B_1)\ \exp(+n_2\{B_2-L_m\})\\
&-(+n_1+b+\ell)\ (-n_2+d+\ell)\\
&\times\exp(+\ell L_m)\ \exp(+n_1B_1)\ \exp(-n_2\{B_2-L_m\})\\
&-(+n_1+b+\ell)\ (-n_2-d-\ell)\\
&\times\exp(+\ell L_m)\ \exp(+n_1B_1)\ \exp(+n_2\{B_2-L_m\})\\
&+(-n_1+b+\ell)\ (-n_2+d+\ell)\\
&\times\exp(+\ell L_m)\ \exp(-n_1B_1)\ \exp(-n_2\{B_2-L_m\})\\
&+(-n_1+b+\ell)\ (-n_2-d-\ell)\\
&\times\exp(+\ell L_m)\ \exp(-n_1B_1)\ \exp(+n_2\{B_2-L_m\})\\
&=0
\end{aligned} \quad (8)$$

where $n_1=[b^2-(2bf/c-\ell^2)]^{1/2}$ (9-1)

$n_2=[d^2+(2df/c+\ell^2)]^{1/2}$ (9-2)

The equation (8) is simplifed as follows:

$$\begin{aligned}
&\ell^2\tanh(\ell L_m)\tanh(n_1B_1)\tanh(n_2\{B_2-L_m\})\\
&+\ell\,\mathrm{tahn}(n_1B_1)\ [n_2+d\tanh(n_2\{B_2-L_m\})]\\
&+\ell\tanh(n_2\{B_2-L_m\})\ [n_1+b\tanh(n_1B_1)]\\
&+\tanh(\ell L_m)\ [n_1+b\tanh(n_1B_1)]\\
&[n_2+d\tanh(n_2\{B_2-L_m\})]=0
\end{aligned} \quad (10)$$

When L_m goes to infinity as shown in Fig. 2 (a), the dispersion relation (10) yields

$$[n_1+(\ell+b)\tanh(n_1B_1)]\cdot[n_2+(\ell+d)\tanh(n_2\{B_2-L_m\})]=0 \quad (11)$$

The above dispersion relation shows two independent sets of continental shelf waves. It means that if the shelves are apart sufficiently enough, two set of continental shelf waves do not interact with each other.

On the other hand, when L_m goes to zero (double shelf case) as shown in Fig. 2 (b), the dispersion relation (10) yields.

$$n_2\tanh(n_1B_1)+n_1\tanh(n_2B_2)+(b+d)\tanh(n_1B_1)\tanh(n_2B_2)=0 \quad (12)$$

This shows the dependences of two sets of shelf waves. It turns out that two sets of shelf waves become independent single shelf waves when the two shelves are separated far enough, while they interact with each other if the two shelves are close enough.

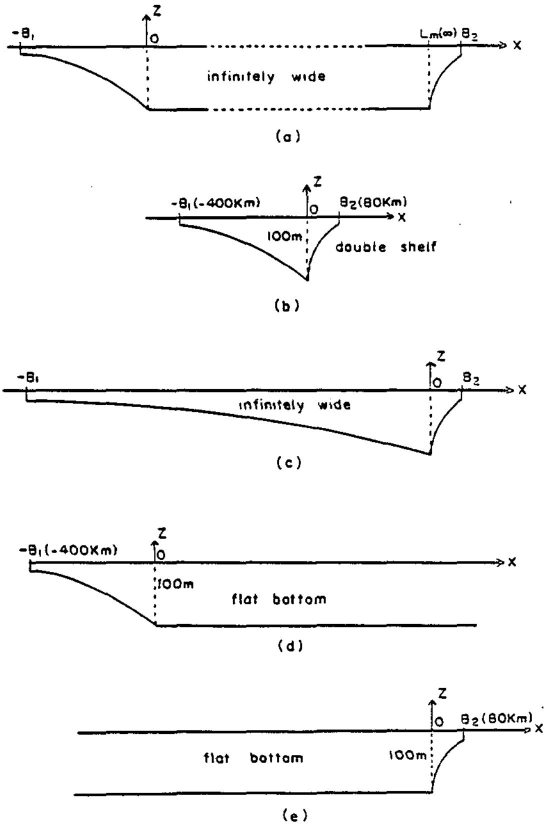

Fig. 2. Schematic representations of the cross shelf sections in various cases (a) two shelves with an infinitely wide intervening region, (b) a double shelf(two adjoining shelves), (c) two shelves with an infinitely wide one shelf, (d) a single shelf of 400*km* width adjoining to a constant depth open ocean. and (e) a single shelf of 80*km* width adjoining to a constant depth open ocean.

Phase Speed

When n_1 and n_2 are real, the equation (10) has only trivial solution, since n_1 and n_2 are positive as defined in (9) and also B_1, L_m and B_2-L_m are positive. In order to have non-trivial solution, n_1 or n_2 must be imaginary. When n_1 is imaginary, $b^2-2bf/c+\ell^2<0$. The frequency ω must obey, for a positive wave number, the inequalty, $0<\omega/f<2b\ell/(b^2+\ell^2)$. The phase speed c is thus positive in the Northern Hemisphere, which implies a southward propagation of waves. Similarly, imaginary n_2 provides the inequality, $-2d\ell/(d^2+\ell^2)<\omega/f<0$. This gives a negative c which implies northward phase propagation. In the above inequality, ω/f goes to zero as ℓ goes both to zero and to infinity. Thus each shelf wave mode has a zero group velocity at some intermediate value of ℓ. For fixed values of the parameter, we can thus find the real solution $\omega_{mn}(\ell)$, m(shelfs)$=1$ and 2, n (mode)$=1, 2, \cdots\cdots$, of the dispersion relation (10). The solutions can be ordered, for a fixed wave number, as

$$-2d\ell/(d^2+\ell^2)<\omega_{21}/f<\omega_{22}/f<\omega_{23}/f<\cdots 0<\cdots$$
$$\cdots\omega_{13}/f<\omega_{12}/f<\omega_{11}/f<2b\ell/(b^2+\ell^2).$$

One set of waves propagates northward and the other propagates southward. The lower the mode, the larger the absolute phase speed. These are comparable to the trench waves (Mysak et al., 1979, 1981) and bank waves (Brink, 1983).

When L_m goes to infinity, (11) yields the dispersion relations for non-trivial solutions, as follows:

$$\tan(n_1B_1)=-n_1/(\ell+b) \qquad (13-1)$$
$$\tan(n_2\{B_2-L_m\})=-n_2(\ell+d) \qquad (13-2)$$

Each of the two dispersion relations in (13) is exactly the same as one obtained by Buchwald and Adams (1968) for a single shelf adjacent to a deep ocean region of constant depth.

The double shelf case also recovers the above limiting cases when one shelf is infinitely wide. In such cases, the dispersion relation (12) yield the above equations (13). For illustration, suppose that B_1 goes to infinity as shown in Fig. 2 (c). Then, b, n_1 and $\tanh(n_1B_1)$ go to, respectively, 0, 1, and 1. (12) exactly reduces to (13−2). (12) shows the dependence of the waves on the bottom topography of both shelves. The appearance of the sum of slope coefficients indicates the constraint of the topography of one shelf on the propagation characteristics of the shelf waves over the other.

The equations (12) can be transformed as follows:

$$\frac{\tanh(n_1B_1)+n_1/(b+d)}{n_1/(b+d)}=\frac{n_2/(b+d)}{\tanh(n_2B_2)+n_2/(b+d)}$$
$$\equiv S \qquad (14)$$

This equation can be rewritten, for non-trivial solutions, such as:

$$\tan(n_1B_1)=(S_1-1)\ \frac{n_1B_1}{(b+d)B_1} \qquad (15-1)$$

$$\tan(n_2B_2) = \left(\frac{1}{S_2} - 1\right)\frac{n_2B_2}{(b+d)B_2} \qquad (15-2)$$

$$\text{where } S_1 = \frac{n_2/(b+d)}{\tanh(n_2B_2) + n_2/(b+d)}$$

$$S_2 = \frac{\tanh(n_1B_1) + n_1/(b+d)}{n_1/(b+d)}$$

To study the solutions of the dispersion relations, (15−1) and (15−2), consider the intersections of the graphs of the both sides. As is illutrated in Fig. 3(an example), there are two infinite sets of intersections, n_{1m} and n_{2m}. The former and the latter subscripts indicate the sets and the modes, respectively. Since n_1B_1 and n_2B_2 are positive, solutions are only in the right hand side. Some topography changes of the any shelf affect the gradient of line, and thus the phase speeds of both sets of waves are changed. This shows the constraint of the topography of the one shelf on the propagation characteristics of the shelf waves over the other.

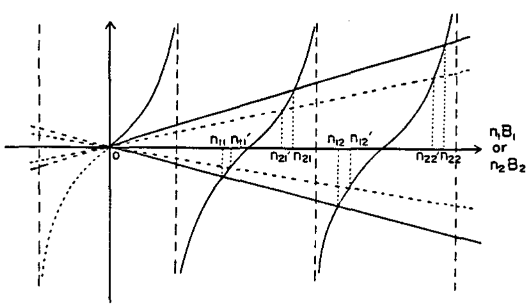

Fig. 3. Graphical Illustraction of two infinitely sets of solutions.

Fig. 4 and 5 show the phase speeds of the first 10 modes in the two sets of shelf waves. One set in Fig. 5 is propagating southward along the shelf 1 and the other set in Fig. 4 is propagating northward along the shelf 2. The shelf widths used in this calculation are 400*km* for shelf 1 and 80*km* for shelf 2 as in Fig. 2 (b). The first mode has the maximum phase speed and thereafter the phase speed decreases in higher mode. Since the phase speed of shelf waves is in some way propotional to shelf width, the phase speed of the southward propagating waves is larger than that of the northward propagating waves.

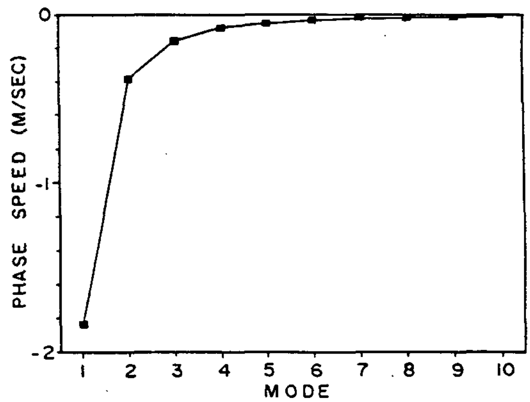

Fig. 4. Phase speeds of the first 10 modes of shelf waves propagating northward.

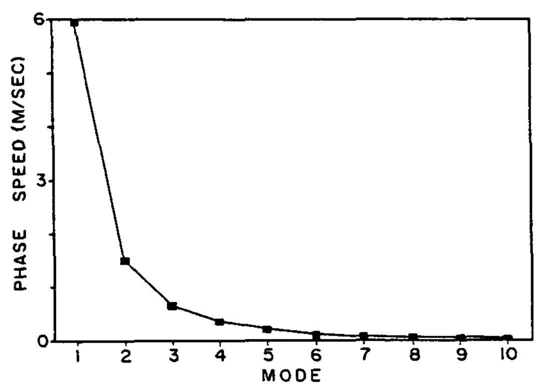

Fig. 5. Phase speeds of the first 10 modes of shelf waves propagating southward.

Fig. 6 and 7 show the comparisons of eigenvalues between a single shelf and a double shelve. The values are listed in Table 1. The single shelf is adjoining to an open ocean of a constant depth. The values of shelf width, used in this calculation, are 400*km* and 80*km*, and the deepest depth is 100 *m*. The cross sections of above two shelves are illustrated in Fig.2 (d) and (e). The first mode in single shelf cases in Table 1 has a tremendous phase speed. The unrealistic phase speeds arise from the non-divergent assumption. This shows that the divegent assumption is necessary for a cross-shelf scale of hundreds meters. The phase speed of the second mode in the single shelf case corresponds to that of the first mode in the double shelf case, and so on. The phase speeds of 80*km*

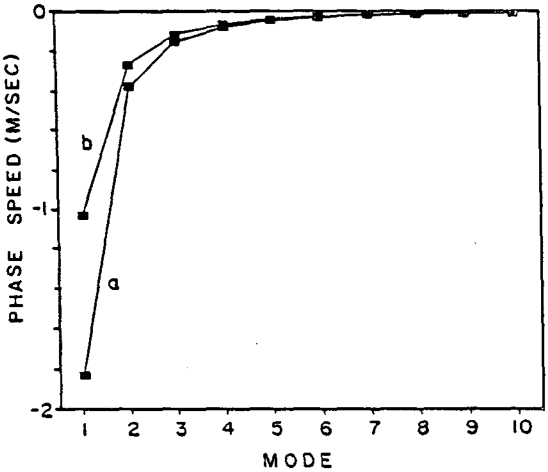

Fig. 6. Comparison of the phase speeds of the northward propagating waves in a double shelf (a) with those of the single shelf waves (b).

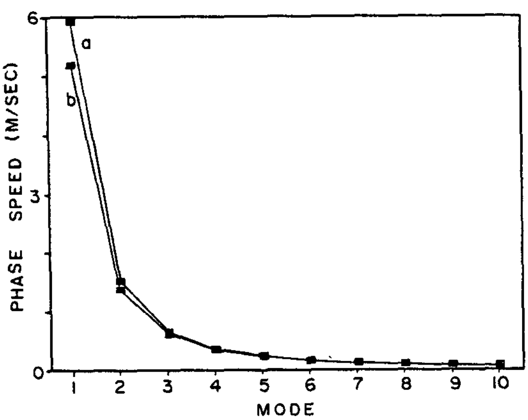

Fig. 7. Comparison of the phase speeds of the southward propagating waves in a double shelf (a) with those of the single shelf waves (b).

shelf have significant influences from the other shelf for a double self case. The results show the effects of bottom topography on the phase speeds.

Eigenfunctions

The eigenfuntions for the eigenvalue problem (6)-(7) are as follows:

$$F=\begin{cases} F_1 & \text{in shelf 1} \\ F_m & \text{in a middle area} \\ F_2 & \text{in shelf 2} \end{cases}$$

Table 1. Eigenvalues of the first 10 modes for the cases of (a) single shelf of 400*km* width, (b) single shelf of 80*km* width, and (c) double shelves of 400*km*~80*km* width. (non-divergent case)

mode	single shelf 400*km*	single shelf 80*km*	double shelf (400~800*km*) 400*km*	double shelf (400~800*km*) 80*km*
1	(83.550)	(-17.278)	5.911	-1.833
2	5.176	- 1.035	1.496	-0.382
3	1.360	- 0.271	0.654	-0.154
4	0.608	- 0.122	0.364	-0.081
5	0.343	- 0.069	0.231	-0.051
6	0.220	- 0.044	0.159	-0.034
7	0.153	- 0.031	0.116	-0.025
8	0.112	- 0.022	0.089	-0.019
9	0.086	- 0.017	0.070	-0.015
10	0.068	- 0.014	0.056	-0.012
11	0.055	- 0.011		

$$F_1=A\,\frac{a1\cdot\exp(\lambda L_2)\cdot(n_2+b_1)+a2\cdot\exp(-\lambda L_2)\cdot(n_2+b_2)}{a2\cdot\exp(-\lambda L_2)\cdot(n_2+b_2)}$$

$$\times\exp(-bx)\,\frac{n_1\cdot\cosh n_1(x+L_1)+(b-1/c)\cdot\sinh n_1(x+L_1)}{n_1\cdot\cosh n_1L_1+(b-1/c)\cdot\sinh n_1L_1}$$

$$F_m=A\,\frac{a1\cdot\exp(-\lambda x)\cdot(n_2+b_1)+a2\cdot\exp\lambda x\cdot(n_2+b_2)}{a2\cdot(n_1+a3\cdot\tanh n_1L_1}$$

$$F_2=A\,\frac{a2\cdot\exp(\lambda L_2)\cdot(n_1+c1)+a1\cdot\exp(-\lambda L_2)\cdot(n_1+c_2)}{a2\cdot\exp(\lambda L_2)\cdot(n_1+c1)}$$

$$\times\exp(-dx)\,\frac{n2\cdot\cosh n_2(L_m-x)+(d+1/c)\cdot\sinh n_2(L_3-x)}{n2\cdot\cosh n_2(L_m-L_2)+(d+1/c)\cdot\sinh n_2(L_m-L_2)}$$

where

$a1=\lambda+1/c$,

$a2=\lambda-1/c$,

$a3=b+\lambda$,

$b1=(d+\lambda)\tanh n_2(L_m-L_2)$,

$b2=(d-\lambda)\tanh n_2(L_m-L_2)$,

$c1=(b+\lambda)\tanh n_1L_1$,

$c2=(b-\lambda)\tanh n_1L_1$. A and λ are, respectively, a arbitrary constant and the Rossby Deformation Radius.

Fig. 8 shows the amplitudes of the first two eigenfunctions across the shelves for each set of shelf waves. The figures (A) and (B) in Fig. 8 represent the continental shelf waves propagating along the shelf 2 and 1, respectively. Thus, the waves in (A) and (B) propagate into and out of the

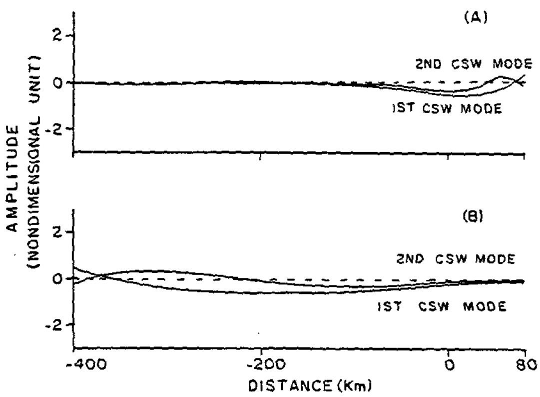

Fig. 8. The amplitudes of the first 2 eigenfunctions of (A) shelf waves propagating northward and (B) shelf waves propagating southward. The shelf widths are 400*km* for shelf 1 and 40*km* for shelf 2.

paper, respectively. The first eigenfunction has 1 node across the shelf and the next mode has 2 nodes and so on. It should be noted that, in the case of single shelf case, the first mode does not hae any node (Clarker and VanGoder, 1986). The southward (northward) propagating waves oscillate over the shelf 1 (shelf 2) and extend in an exponentially decay over the shelf 2 (shelf 1).

When the horizontal divergence terms are not included in the equations, there is no Kelvin wave in the solution whose amplitude has no node in the cross-shelf direction. However, we do not have any analytical solution in a horizontal divergence case with an exponential topography. That is why many reports, including this report, do not have the first mode of no node. It does not mean that there is no such a mode. Physically, it is quite natural to have the mode in real oceans. Over a double shelf topography, we also have those modes for a horizontal divergence case with a linear topography (Hsueh & Pang, 1989).

Conclusions

The bottom topography as in Fig. 1 allows the existence of two sets of waves propagating in opposite directions. These are comparable to the trench waves (Mysak et al., 1979, 1981) and bank waves (Brink, 1983). In the case that two shelves are apart sufficiently, the solutions show two independent sets of waves which recover the single shelf waves shown by Buchwald and adams (1968). However, over a double shelf in which two shelves ard adjoining each other, the waves become dependent on the geometry of both shelves. The dispersion relation shows the constraint of the topography of the one shelf on the propagation characteristics of the shelf waves over the other. The comparisons of phase speeds between a single shelf and a double shelf clearly show the influences of the bottom topography of the other shelf.

Even over a double shelf topography, shelf waves propagate with the shallow water to the right in the Northern Hemisphere. The group velocity of shelf wave has the same direction as phase velocity in the long wave case, but the opposite direction in the short wave case. Thus, each shelf mode has a zero group velocity at some intermediate value of wave length. It means that the basic characteristics of continental shelf waves are not changed by the bottom topography.

The first eigenfunction over a double shelf topography has one node for a non-divergnece case, while it does not have any node for a horizontal divergence case. For a single shelf case, the first mode has no node too if the horizontal divergence terms are included. The amplitude of shelf waves oscillate over one shelf and extend in an exponentially decay over the other shelf. Therefore, the continental shelf wave energy over a double shelf is mostly confined to the shelf along which the wave propagates.

References

Brink, K. H., 1983. Low-frequency free wave and wind-driven motions over a submarine bank. J. Phys. Oceanogr., 13, 103~116.

Brink, K. H., and J. S. Allen, 1978. On the effect of bottom friction on barotropic motion over the continental shelf. J. Phys. Oceanogr., 8, 919~922.

Buchwald, V. T., and J. K. Adams, 1968. The propagation of continental shelf waves. Proc.

Roy. Soc. London, A305, 235~250.

Clarke, A. J., and S. Van Gorder, 1986. A method for estimating wind-driven frictional time-depenadent, stratified shelf and slope water flow. J. Phy. Oceanogr., 16, 1013~1028.

Gill, A. J., and E. H. Schumann, 1974. The generation of long shelf waves by the wind. J. Phys. Oceanogr., 4, 83~90.

Hsueh, Y., and I. C. Pang, 1989. Coastally trapped long waves in the Yellow Sea. J. Phys. Oceanogr., 19, 5, 612~625.

Huthnance, J. M., 1975. On trapped waves over a continental shelf. J. Fluid Mech., 67, 689~704.

Huthnance, J. M., 1978. On coastal trapped waves: Analysis and calculation by inverse iteration. J. Phys. Oceanogr., 8, 74~92.

LeBlond, P. H., and L. A. Mysak, 1978. Waves in the Oceans. Elsevier. 602pp.

Louis, J. P., 1978. Low-frequency edge waves over a trench-ridge topography adjoining a straight coastline. Geophys. Astrophys. Fluid Mech., 55, 113~127.

Mitchum, G. T., and A. J. Clarke, 1986. The frictional nearshore response to forcing by synoptic scale winds. J. Phys. Oceanogr., 16, 934~946.

Mysak, L. A., and P. H. LeBlond, and W. J. Emery, 1979. Trench waves. J. Phys. Oceanogr., 9, 1001~1013.

Mysak, L. A., 1980, Recent advences in shelf wave dynamics. Rev. Geophys. Space Phys., 18, 211~241.

Mysak, L. A., and A. J. Willmott, 1981. Forced trench waves. J. Phys. Oceanogr., 11, 1481~1502.

Pang, I. C., 1987. Theory of coastally trapped waves and its application to the Yellow Sea. Ph. D. Dissertation. Florida State Uniersity, 128pp.

Received October 5, 1991
Accepted November 13, 1991

Ig-Chan PANG

양향성 대륙붕의 대륙붕파(Ⅰ): 지수함수적 해저지형에서의 자유파

방 익 찬
제주대학교 해양학과

영향성 대륙붕에서는 서로 반대 방향으로 진행하는 두 집합의 대륙붕파가 생성된다. 두 대륙붕이 충분히 떨어질 경우에는 두 집합의 대륙붕파는 독립된 대륙붕파가 되며 이 파들은 하나의 대륙붕 지형의 대륙붕파와 일치한다. 그러나 두 대륙붕의 간격이 Rossby Deformation Radius 보다 가까울 때는 두 집합의 대륙붕파는 두 대륙붕 지형에 영향을 받게 된다.

영향성 대륙붕에서도 대륙붕파는 북반구에서 해안선을 오른쪽에 두고 진행한다. 군속도(group velocity)는 장파인 경우에는 파의 진행방향과 같으나 단파인 경우에는 반대가 된다. 그러므로 각 대륙붕파는 어떤 중간의 파장에서 0인 군속도를 갖게 된다.